Effects of miR-93 on epithelial-to-mesenchymal transition and vasculogenic mimicry in triple-negative breast cancer cells

GAILI AN[1,2], FENG LU[2], SHANGKE HUANG[3], JUN BAI[1], LI HE[1], YI LIU[1] and LEI HOU[1]

[1]Department of Clinical Oncology, Shaanxi Provincial People's Hospital, Xi'an, Shaanxi 710068;
[2]Department of Oncology, The First Affiliated Hospital of Xi'an Jiaotong University, Xi'an, Shaanxi 710061;
[3]Department of Oncology, The Affiliated Hospital of Southwest Medical University, Luzhou, Sichuan 646000, P.R. China

Abstract. Triple-negative breast cancer (TNBC) is characterized by strong invasiveness, frequent local recurrence and distant metastasis, with poor prognosis. According to tumor angiogenesis theory, tumor cells can obtain blood supply not only by fusing with host blood vessels, but also by constructing a new vascular system through angiogenesis, so as to continuously obtain nutrients and oxygen supply; this is called vasculogenic mimicry (VM). In our previous study, differential expression profiles of miRNAs were examined with gene chip in TNBC and corresponding paracancer tissues, which demonstrated significant up-regulation of microRNA (miR)-93. Bioinformatics found that the target genes of miR-93 were associated with cell proliferation, invasion and migration. The present study investigated the association between miR-93, epithelial-to-mesenchymal transition (EMT) and VM formation in TNBC cell lines. The results indicated that miR-93 depletion suppressed MDA-MB-231 cell viability, invasion and migration (P<0.001). In addition, knockdown of miR-93 significantly upregulated the expression levels of EMT-associated genes such as E-cadherin and occludin, but downregulated the expression levels of vimentin and N-cadherin in MDA-MB-231 cells. VM formation assay showed a significant decrease in microtubule-forming ability of cells following miR-93 knockdown, which was associated with the occurrence of EMT, suggesting that miR-93 may promote the formation of VM via EMT and may be a therapeutic target for the treatment of TNBC.

Correspondence to: Dr Lei Hou, Department of Clinical Oncology, Shaanxi Provincial People's Hospital, 277 Youyi Western Road, Xi'an, Shaanxi 710068, P.R. China
E-mail: zhaoyalan1981@163.com

Introduction

Triple-negative breast cancer (TNBC), as a molecular subtype of breast cancer, is susceptible to early recurrence and metastasis. Patients with TNBC have poor prognosis owing to a lack of effective clinical treatment measures (1). Tumor cells receive blood supply by fusion with the host blood vessels, as well as by vascular formation methods, such as constructing new vascular systems, which is called vasculogenic mimicry (VM) (2). This phenomenon was discovered by Maniotis *et al* (2), who studied the microcirculation of human uveal melanoma and demonstrated a novel manner by which tumor cells obtain blood supply. According to the VM theory, when the tumor diameter is >2 mm, vascular endothelial cells are activated to construct new blood vessels to obtain blood supply to prevent tumor cell necrosis as a result of ischemia and hypoxia (1). The VM theory suggests that tumor cells form tubular structures, and it has been hypothesized that tumor cells exhibit stem cell plasticity, similar to the phenotype and function of endothelial cells, and can differentiate into endothelial cells in the tumor microenvironment (3,4). VM has been reported in melanoma, glioma and bidirectional malignancy, as well as colon, liver, ovarian, bladder and prostate cancer (5-10). A previous study found that VM also exists in TNBC, and that VM formation and high expression levels of CD133$^+$ may be primary reasons for recurrence and progression of TNBC (11).

Epithelial-to-mesenchymal transition (EMT) refers to the process by which epithelial cells lose their polarity and cell-cell contacts to acquire certain characteristics of mesenchymal cells (12). EMT serves an important role in the invasion and the metastasis of numerous types of cancer, including breast and colorectal cancer (13,14). The expression levels of E-cadherin and occludin are downregulated, whereas the expression levels of N-cadherin and vimentin are upregulated during EMT (15).

MicroRNAs (miRNAs or miRs) are non-coding RNAs that serve important roles in regulating the expression levels of mRNAs. Aberrant miRNAs are known to act as promoters or inhibitors of EMT (16). miR-93 is a member of the miR-106b-25 cluster (17). Overexpression of miR-93 has been identified in multiple types of cancer, including hepatocellular, gastric and breast cancer, as well as glioma and endometrial carcinoma, in which it serves as an oncogene (17). The expression levels of miR-93 have been demonstrated to be markedly

increased in TNBC tissue compared with non-TNBC tissue, and are associated with clinicopathological features, such as increased lymph node metastasis, higher TNM staging and increased Ki-67 expression (18), indicating that miR-93 contributes to cell proliferation and metastasis. Moreover, miR-93 is involved in the process of EMT in endometrial carcinoma and breast cancer cells (19,20). However, the regulatory mechanism of miR-93 on EMT and VM in TNBC remains unclear. Therefore, the present study investigated the role and underlying mechanism of miR-93 in EMT transformation and VM formation to provide a potential therapeutic target for TNBC.

Materials and methods

Cell culture. Human breast cancer cell lines MDA-MB-231, SK-BR-3 and MCF-7 were donated by The Medical Center Laboratory of Xi'an Jiaotong University (Xi'an, China) and cultured in RPMI-1640 and DMEM (Gibco; Thermo Fisher Scientific, Inc.) at 37˚C. Non-tumorigenic MCF-10A cells were purchased from The Cell Bank of Type Culture Collection of the Chinese Academy of Sciences and cultured in McCoy's 5A medium (Gibco; Thermo Fisher Scientific, Inc.). All media were supplemented with 10% FBS (Biological Industries), along with 1% penicillin and streptomycin.

miR-93 RNA interference (RNAi). MDA-MB-231 cells were seeded in a 6-well plate at $5x10^4$ cells/well for RNAi. Cells were then divided into lentivirus-short hairpin (sh)RNA and negative control (shNC) groups, in which cells were infected with the miR-93 knockdown recombinant (5'-CTACCTGC ACGAACAGCACTTTG-3') and empty green fluorescent protein (GFP) lentivirus (5'-TTCTCCGAACGTGTCACGT-3'), respectively. Lentiviral vectors were constructed by Shanghai GeneChem Co., Ltd. Cells were infected with shNC and shRNA lentiviral particles (multiplicity of infection, 10) and incubated for 8 h at 37˚C. The medium containing lentiviruses was then removed, and cells were cultured in normal culture medium for another 12 h. Subsequently, 72 h after infection, the expression levels of GFP were observed through a fluorescent microscope (magnification, x100; data not shown). Cells with infection efficiency >80% were selected for subsequent analysis.

MTT assay. Following digestion by trypsin, MDA-MB-231 cells in logarithmic growth phase were resuspended in complete medium (RPMI-1640 medium supplemented with 10% FBS and 1% penicillin and streptomycin). Cells were plated at a density of $5x10^3$ cells/well into 96-well plates. Following incubation at 37˚C for 48 h, 20 μl MTT reagent (5 mg/ml) was added to each well and incubated at 37˚C for 4 h. Finally, 100 μl dimethyl sulfoxide was added to completely dissolve the purple formazan crystals. The absorbance of each well was measured at 492 nm using a multi-functional microplate reader for evaluation of cell viability.

Western blot analysis. Total cellular protein was extracted using RIPA buffer (Beyotime Institute of Biotechnology) and the protein concentrations were determined by a BCA Protein Assay kit (Pierce; Thermo Fisher Scientific, Inc.) according to

the manufacturer's instructions. Each sample contain 50 μg of protein was separated by 10% SDS-PAGE, the proteins were transferred to PVDF membrane and blocked with 5% non-fat milk at 37˚C for 1 h. The blots were incubated overnight with specific primary antibodies (anti-E-cadherin; cat. no. 4065; Cell Signaling Technology, Inc., anti-N-cadherin; cat. no. ab76057, Abcam, anti-vimentin; cat. no. 5741, Cell Signaling Technology, Inc. and anti-occludin; cat. no. 71-1500, Invitrogen (Thermo Fisher Scientific, Inc.); all at a dilution of 1:1,000) at 4˚C and thereafter with the HRP-conjugated secondary antibody (dilution of 1:1,000, goat anti-rabbit, cat. no. sc-2004; goat anti-mouse; cat. no. sc-2005, Santa Cruz Biotechnology, Inc.) for 1 h at room temperature. ECL reagent (EMD Millipore) was used to detect protein expression levels that were analyzed with Quantity One 6.0 software (Bio-Rad Laboratories, Inc), and the protein expression levels were normalized to β-actin.

RNA extraction and reverse transcription-quantitative PCR (RT-qPCR). Total RNA was extracted from the cell lines using TRIzol® (Thermo Fisher Scientific, Inc.). The RNA samples were diluted with sterile water, and the absorbance values at 260 and 280 nm were detected using a spectrophotometer; a 260/280 value of 1.8-2.0 indicated optimal RNA quality. cDNA was synthesized using the isolated RNA as a template by PrimeScript RT reagent kit (Fermentas; Thermo Fisher Scientific, Inc.) according to the manufacturer's protocol. The SYBR Green PCR kit (Takara Biotechnology Co., Ltd.) was used to perform qPCR. The thermocycling conditions were: 95˚C for 10 sec, followed by 40 cycles of 95˚C for 5 sec, 60˚C for 30 sec, one cycle of 95˚C for 15 sec, 60˚C for 30 sec. Melting curve analysis was used to confirm specificity of the PCR products. Relative expression levels of the detected genes were assessed using the $2^{-\Delta\Delta Cq}$ method (21). GAPDH was used as an internal control for mRNA, and U6 was an internal control for miRNA. The primers used are listed in Table I.

Cell migration and invasion assay. For the cell migration assay, equal numbers of cells ($1x10^5$ cells/ml) were seeded in the top compartment of a 24-well chamber in 200 μl serum-free RPMI-1640. Additionally, 600 μl medium containing 10% FBS was added into the bottom chamber of the system. The cells were incubated at 37˚C for 24 h. After carefully removing the non-migrated cells on the upper surface of the Transwell chamber membrane, the cells that had migrated from the membrane were fixed with 4% paraformaldehyde for 30 min followed by staining with 0.1% crystal violet for 10 min, both at room temperature. The number of migrated cells was counted from five random fields of view under an inverted phase-contrast microscope (magnification, x200). Cell invasion assays were performed in the same way as migration assays except that the cells were seeded in the upper compartment of the chamber and the membrane was pre-coated with diluted Matrigel for 30 min at 37˚C.

VM. Matrigel was added into 48-well plates at 100 μl/well, and then incubated at 37˚C for 30 min. Cells ($2x10^4$ cells/ml) were added to each well. Following incubation at 37˚C for 12 h, cells with tubular structure formation were imaged using an inverted microscope, and the number of tubular cells

Table I. Primer sequences used for RT-quantitative PCR.

| Gene	Primer name	Primer sequence (5'→3')
Hsa-miR-93	miR-93 RT	GTCGTATCCAGTGCA GGGTCCGAGGTATTCGCACTGGATACGACCTACCT
	Forward	ATTCGGCAAAGTGCTGTTCGTGC
	Reverse	ATCCAGTGCAGGGTCCGAGG
U6	U6 RT	GTCGTATCCAGTGCA GGGTCCGAGGTATTC GCACTGGATACGACAAAATA
	Forward	AGAGAAGATTAGCATGGCCCCTG
	Reverse	GTGCAGGGTCCGAGGT
E-cadherin	Forward	GATTCCTTGCCAGTTGGTGT
	Reverse	TTCCTGCCTGGATTGGTATC
N-cadherin	Forward	TTCTGGCTGTTGTGTTGAGG
	Reverse	ATTCCACCGCTACCACTTTG
Vimentin	Forward	TGCCTCAACCTCCCAAGTAG
	Reverse	GGTCAGGAGTTCGAGACCAG
GAPDH	Forward	ATCTGGCACCACACCTTCTACAATGAGCTGCG
	Reverse	CGTCATCCCTGCTTGCTGATCCACATC

RT, reverse transcription.
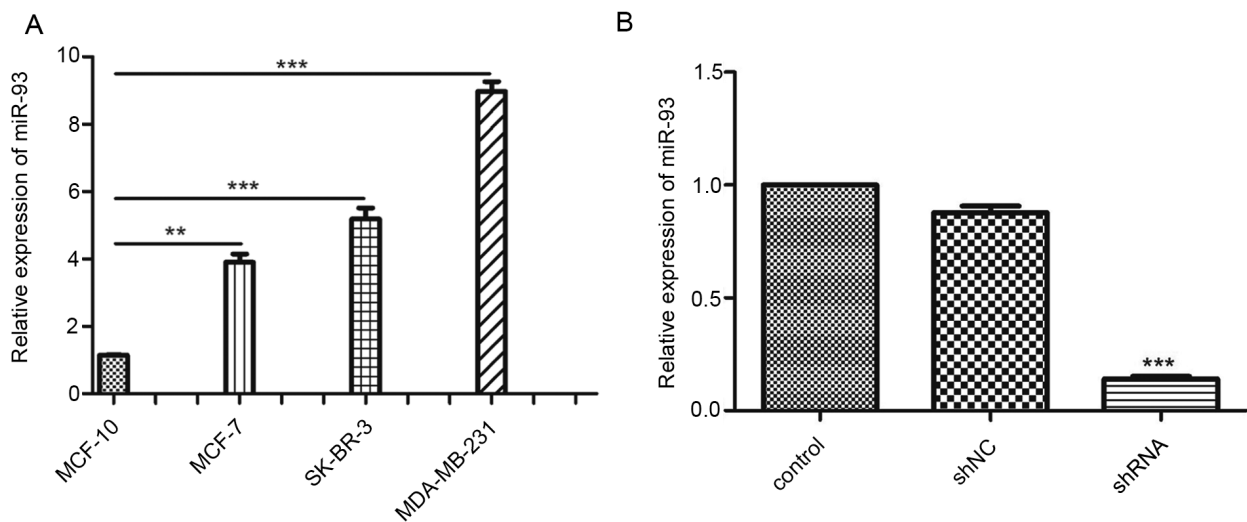
Figure 1. miR-93 expression significantly different in breast cancer cell lines and knockdown of miR-93 using shRNA. (A) Expression levels of miR-93 in breast cancer cell lines was detected by RT-qPCR. **P<0.01, ***P<0.001 vs. MCF-10; (B) RT-qPCR confirmed that expression levels of miR-93 were significantly inhibited by shRNA. ***P<0.001 vs. shNC. miR, microRNA; NC, negative control; RT-qPCR, reverse transcription-quantitative PCR; sh, short hairpin RNA.

(completely surrounded by a circle) were counted manually from five random visual fields (up, down, left, right and center) to calculate the average. Following incubation at 37°C for 48 h, cells were digested with dispase and recycled with cell recovery solution, which enables recovery of cells cultured on Matrigel for subsequent biochemical analysis of PCR and western blot.

Statistical analysis. All data are presented as the mean ± standard deviation of at least three independent repeats. SPSS 19.0 software (IBM Corp.) was used for statistical analysis. Data were analyzed by unpaired Student's t-test or one-way ANOVA followed by Tukey's or Fisher's least significant difference post

hoc test, as appropriate. P<0.05 was considered to indicate a statistically significant difference.

Results

miR-93 expression levels in breast cancer cell lines and knockdown of miR-93 using shRNA. The expression levels of miR-93 in MCF-7, SK-BR3, MDA-MB-231 and non-tumorigenic MCF-10A cell lines were detected by RT-qPCR. The results showed that the expression levels of miR-93 were significantly higher in the three breast cancer cell lines compared with expression in MCF-10A cells (P<0.01 and P<0.001; Fig. 1A), with the highest expression in MDA-MB-231 cells. Hence,

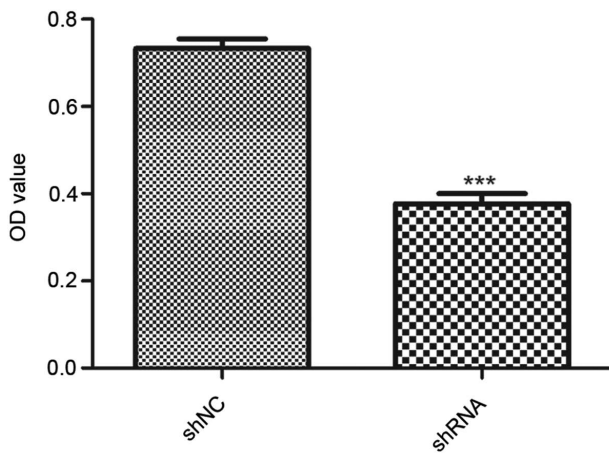Figure 2. MTT results indicated that the viability of cells in the miR-93 shRNA group was significantly decreased. ***P<0.001 vs. shNC. miR, microRNA; NC, negative control; OD, optical density; sh, short hairpin RNA.

the MDA-MB-231 cell line was chosen for subsequent experiments. RT-qPCR confirmed that expression of miR-93 was significantly inhibited by miR-93 shRNA (P<0.001; Fig. 1B).

miR-93 depletion decreases MDA-MB-231 breast cancer cell viability. The effect of miR-93 on the viability of MDA-MB-231 cells was determined by MTT assay. Results showed a statistically significant decrease in optical density in the shRNA group compared with the shNC group (P<0.001; Fig. 2), suggesting that downregulation of miR-93 suppressed the viability of MDA-MB-231 cells.

miR-93 depletion contributes to cell migration and invasion. The Transwell assays revealed the effects of miR-93 knockdown on the migratory and invasive activity of MDA-MB-231 cells. Compared with the control (209.3±7.2 cells/field) and shNC groups (202.0±8.7 cells/field), cell migration was significantly decreased in the shRNA group (88.8±5.0 cells/field; both P<0.001; Fig. 3). Compared with the control (129.6±8.4 cells/field) and shNC groups (112.0±4.7 cells/field), cell invasion was also significantly decreased in the shRNA group (68.8±7.0 cells/field; both P<0.001; Fig. 3). Cell migration and invasion were not significantly different between the control and shNC groups (both P>0.05; Fig. 3). These results showed that the migratory and invasive ability of MDA-MB-231 cells decreased following miR-93 depletion.

miR-93 depletion alters expression levels of EMT-associated markers in MDA-MB-231 breast cancer cells. The association between miR-93 and EMT markers was analyzed. RT-qPCR and western blotting were used to detect changes in the expression levels of EMT-associated markers (E-cadherin, N-cadherin, vimentin and occludin) following miR-93 depletion. RT-qPCR results showed that miR-93-knockdown cells displayed increased mRNA expression levels of E-cadherin and occludin and decreased mRNA expression levels of N-cadherin and vimentin (P<0.001; Fig. 4A). Western blot assay results were consistent with the RT-qPCR and showed that the protein expression levels of E-cadherin and occludin

were significantly upregulated, whereas the protein expression levels of N-cadherin and vimentin were significantly downregulated in the shRNA group compared with the respective expression levels in the shNC group (P<0.01; Fig. 4B and C). These results suggested that knockdown of miR-93 may inhibit the EMT process in MDA-MB-231 cells.

miR-93 depletion suppresses VM formation in MDA-MB-231 breast cancer cells. Vascularization was observed with an inverted microscope in three-dimensional culture of MDA-MB-231 cells following miR-93 knockdown. VM was observed in all three groups (Fig. 5A). The results showed that the microtubule-forming ability of cells was significantly decreased in the shRNA group compared with the control and the shNC groups (P<0.01; Fig. 5B), suggesting that miR-93 may serve as a promoter of VM formation in MDA-MB-231 cells.

miR-93 depletion inhibits expression levels of EMT-associated markers in three-dimensional cell culture. To determine whether knockdown of miR-93 affects the EMT process in three-dimensional culture of MDA-MB-231 cells, western blotting (Fig. 6A) and RT-qPCR (Fig. 6B) were performed. The results indicated that the mRNA and protein expression levels of E-cadherin increased, whereas those of vimentin decreased in the shRNA group compared with the shNC group, suggesting that miR-93 may promote VM formation through the EMT process (P<0.01 and P<0.001).

Discussion

miR-93, a member of the miR-106b-25 cluster, is located on intron 13 of the MCM 7 gene on chromosome 7q22. Studies have previously reported that the miR-106b-25 cluster is highly expressed in esophageal, gastrointestinal, liver, prostate and endometrial cancer, suggesting that it may be a potential proto-oncogene (22-24). Lowery *et al* (25) showed that the expression profile of miRNAs is associated with the hormone receptor status in breast cancer and may be an important indicator for the molecular classification, clinical diagnosis, treatment choice and prognosis. Cascione *et al* (26) found that the expression profiles of miRNAs and mRNAs are associated with the survival of patients with TNBC; miR-16, miR-155, miR-125b and miR-374a are associated with survival, and miR-16, miR-125b, miR-374a, miR-374b, miR-421, miR-655 and miR-497 are associated with disease-free survival. Multi-factor analysis has suggested that the aforementioned indicators are independent prognostic factors that affect the survival of patients. Nam *et al* (27) found that compared with normal ovarian tissue, miR-93 expression levels are significantly increased in ovarian cancer tissue, and that this is associated with worse prognosis. In our previous study (28) gene chip technology was used to investigate the differential expression profiles of miRNAs in TNBC compared with corresponding paracarcinoma tissue; the results demonstrated a significant upregulation of miR-93. The target genes of miR-93 were predicted using bioinformatics and found that these target genes promoted cell viability, invasion and migration (28). Our earlier work confirmed that miR-93 expression is increased in clinical specimens of patients with TNBC and
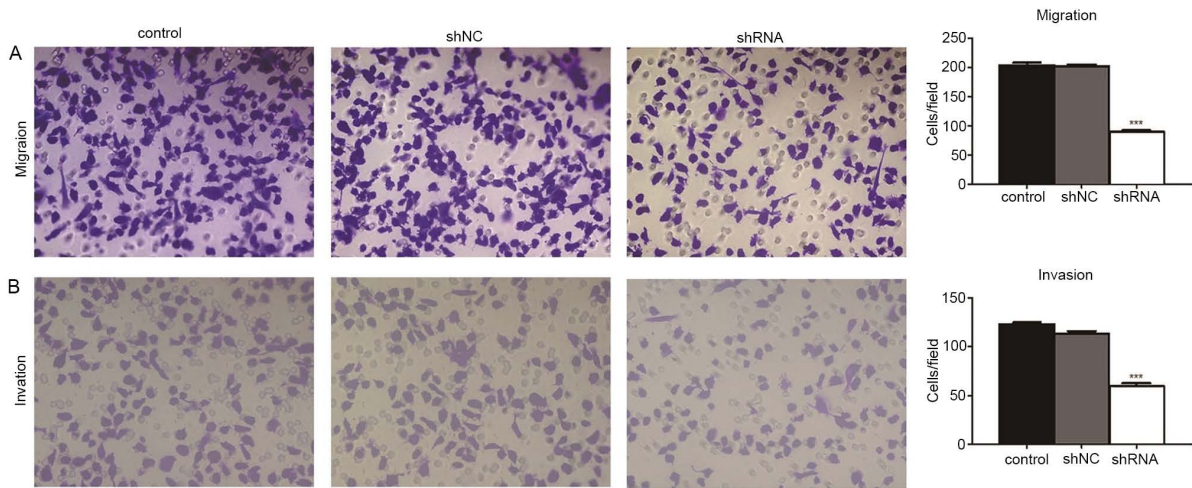
Figure 3. miR-93 depletion contributes to cell migration and invasion (A) migration and (B) invasion of MDA-MB-231 cells decreased following miR-93 depletion. Magnification, x200. ***P<0.001 vs. shNC. miR, microRNA; NC, negative control; sh, short hairpin.
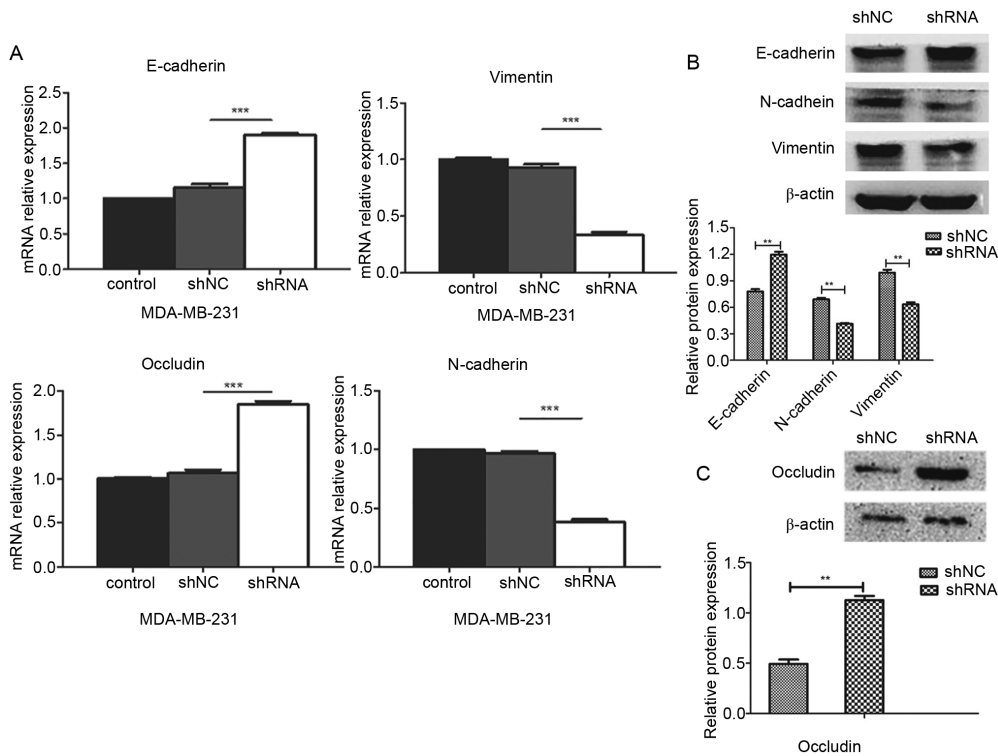

Figure 4. miR-93 depletion alters expression levels of EMT-associated markers. (A) Reverse transcription-quantitative PCR and (B and C) western blotting were performed to measure the expression levels of EMT-related markers E-cadherin, N-cadherin, vimentin and occludin. **P<0.01, ***P<0.001. EMT, epithelial-to-mesenchymal transition; NC, negative control; sh, short hairpin RNA.

that this is associated with poor prognosis (high TNM staging and lymph node metastasis) (29). The present study confirmed at the cytology level that miR-93 depletion inhibited the viability of TNBC cells, and decreased cell invasion and migration, which was consistent with the results of previous experiments using clinical specimens.

miRNAs are involved in the formation of VM. Weng *et al* (30) found that miR-409-3p inhibits VM formation in human fibrosarcoma cells. Wu *et al* (31) demonstrated that miR-26b directly regulates the expression levels of Ephrin type-A receptor 2 to inhibit VM formation in glioma.

Shevde *et al* (32) confirmed that miR-299-5p is associated with VM formation in breast cancer. In the present study, miR-93 depletion was found to inhibit the formation of VM in three-dimensional culture of MDA-MB-231 cells, which was consistent with the results of the aforementioned studies.

EMT refers to the process by which epithelial cells acquire specific characteristics of mesenchymal cells. Mani *et al* (13) found that mammary epithelial cells that underwent the EMT process acquired certain characteristics of stem cells, such as increased tumorigenesis. Liu *et al* (14)
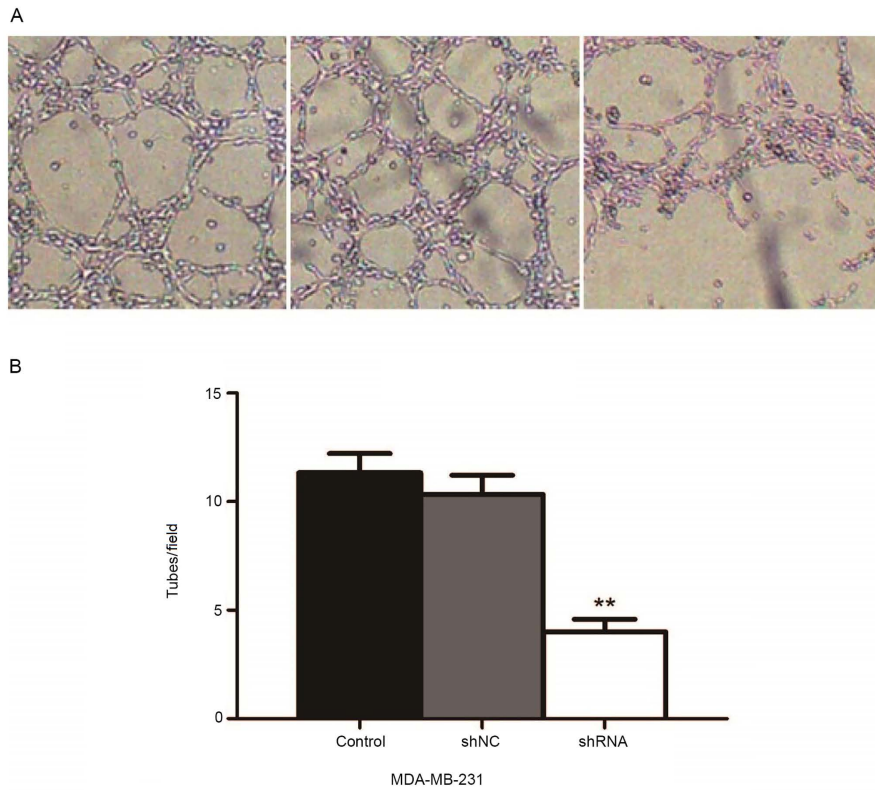
Figure 5. miR-93 depletion suppresses VM formation. (A) VM of MDA-MB-231 cells was observed by microscopy; magnification, x100. (B) Number of tubular structures in MDA-MB-231 cells following microRNA-93 depletion by shRNA. **P<0.01 vs. shNC. NC, negative control; sh, short hairpin; VM, vasculogenic mimicry.
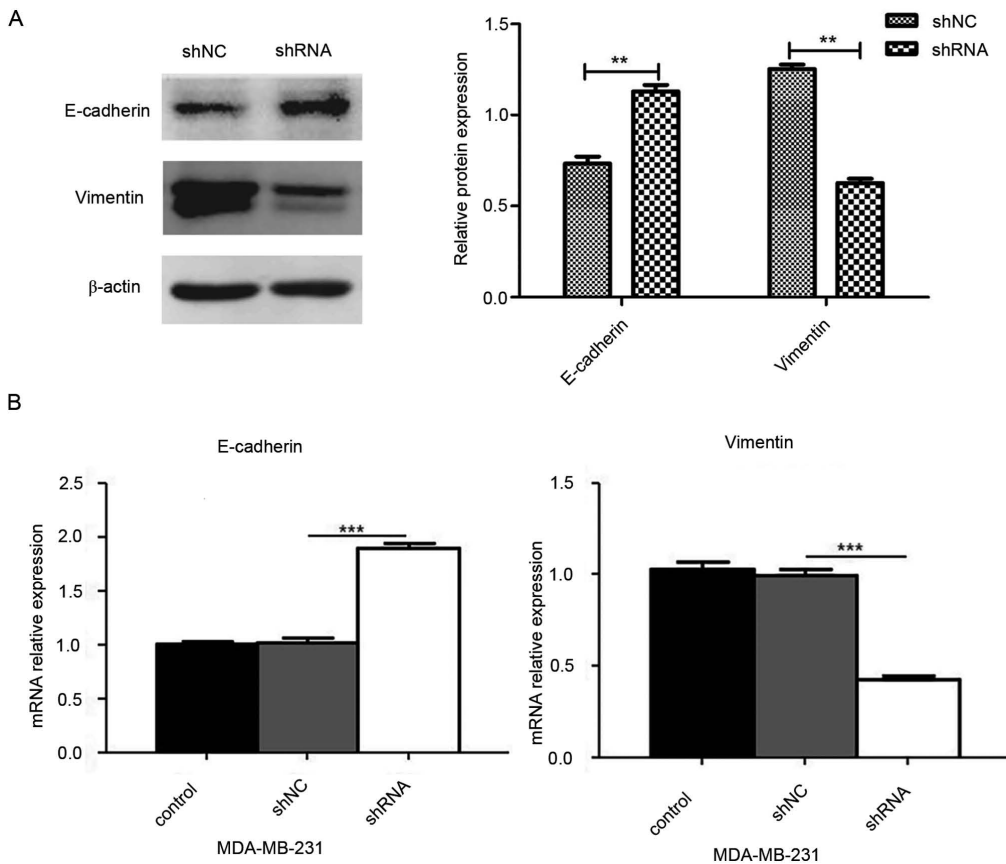

Figure 6. Expression of E-cadherin and vimentin in three-dimensional cell culture following microRNA-93 depletion by shRNA. (A) Western blotting and (B) reverse transcription-quantitative PCR were performed to measure the protein and mRNA expression levels, respectively. **P<0.01, ***P<0.001. NC, negative control; sh, short hairpin RNA.

reported high expression levels of zinc-finger E-box binding homeobox 1 (ZEB1) in VM-positive colon cancer tissue and that expression levels of E-cadherin are decreased, whereas those of vimentin are increased in ZEB1-positive tissue. Moreover, the formation of VM in colon cancer significantly decreases following downregulation of ZEB1 (14). Sun *et al* (33) observed a significant decrease in VM formation following downregulation of Twist-related protein 1 in liver cancer. The present study showed that miR-93 depletion significantly increased the protein expression levels of E-cadherin and occludin and decreased those of N-cadherin and vimentin in monolayer cell culture, suggesting that miR-93 may promote the occurrence of EMT in TNBC cells. Moreover, in the shRNA group VM was inhibited and the expression levels of E-cadherin were higher, whereas the expression levels of vimentin were lower in three-dimensional cell culture, suggesting that miR-93 may promote the formation of VM through the EMT process.

VM determines the ability of tumor cells to form blood cavities, which is associated with poor prognosis in patients with TNBC (34). Lack of experimentation on non-TNBC cell lines is a limitation of the present study; further investigations involving both TNBC and non-TNBC cell lines are required to determine if the effects of miR-93 specifically act on the TNBC subtype. In summary, the present study demonstrated that knockdown of miR-93 inhibited the formation of VM in MDA-MB-231 TNBC cells and this was associated with the expression levels of EMT markers. Therefore, targeting miR-93 may provide a novel option for the anti-angiogenic treatment of TNBC.

Acknowledgements

Funding

Availability of data and materials

The datasets used and/or analyzed during the current study are available from the corresponding author on reasonable request.

Authors' contributions

GA, FL, SH, YL and LHo performed all the experiments. GA, LHe, JB and LHo designed the experiments. GA and FL analyzed the data. GA, FL and LHo wrote the manuscript. All authors read and approved the final manuscript.

Ethics approval and consent to participate

Not applicable.

Patient consent for publication

Not applicable.

Competing interests

The authors declare that they have no competing interests.

References

1. Anders C and Carey LA: Understanding and treating triple-negative breast cancer. Oncology (Williston Park) 22: 1233-1239, discussion 1239-1240, 1243, 2008.
2. Maniotis AJ, Folberg R, Hess A, Seftor EA, Gardner LM, Pe'er J, Trent JM, Meltzer PS and Hendrix MJ: Vascular channel formation by human melanoma cells in vivo and in vitro: Vasculogenic mimicry. Am J Pathol 155: 739-752, 1999.
3. Hendrix MJ, Seftor EA, Hess AR and Seftor RE: Vasculogenic mimicry and tumour-cell plasticity: Lessons from melanoma. Nat Rev Cancer 3: 411-421, 2003.
4. Paulis YWJ, Soetekouw PMMB, Verheul HMW, Tjan-Heijnen VC and Griffioen AW: Signalling pathways in vasculogenic mimicry. Biochim Biophys Acta 1806: 18-28, 2010.
5. McDonald DM and Foss AJ: Endothelial cells of tumor vessels: Abnormal but not absent. Cancer Metastasis Rev 19: 109-120, 2000.
6. Sood AK, Seftor EA, Fletcher MS, Gardner LM, Heidger PM, Buller RE, Seftor RE and Hendrix MJ: Molecular determinants of ovarian cancer plasticity. Am J Pathol 158: 1279-1288, 2001.
7. Shirakawa K, Kobayashi H, Heike Y, Kawamoto S, Brechbiel MW, Kasumi F, Iwanaga T, Konishi F, Terada M and Wakasugi H: Hemodynamics in vasculogenic mimicry and angiogenesis of inflammatory breast cancer xenograft. Cancer Res 62: 560-566, 2002.
8. Sharma N, Seftor RE, Seftor EA, Gruman LM, Heidger PM Jr, Cohen MB, Lubaroff DM and Hendrix MJ: Prostatic tumor cell plasticity involves cooperative interactions of distinct phenotypic subpopulations: Role in vasculogenic mimicry. Prostate 50: 189-201, 2002.
9. Hao X, Sun B, Zhang S and Zhao X: Microarray study of vasculogenic mimicry in bi-directional differentiation malignant tumor. Zhonghua Yi Xue Za Zhi 82: 1298-1302, 2002 (In Chinese).
10. Dupuy E, Hainaud P, Villemain A, Bodevin-Phèdre E, Brouland JP, Briand P and Tobelem G: Tumoral angiogenesis and tissue factor expression during hepatocellular carcinoma progression in a transgenic mouse model. J Hepatol 38: 793-802, 2003.
11. Zhang D, Sun B, Zhao X, Ma Y, Ji R, Gu Q, Dong X, Li J, Liu F, Jia X, et al: Twist1 expression induced by sunitinib accelerates tumor cell vasculogenic mimicry by increasing the population of CD133+ cells in triple-negative breast cancer. Mol Cancer 13: 207, 2014.
12. Shook D and Keller R: Mechanisms, mechanics and function of epithelial-mesenchymal transitions in early development. Mech Dev 120: 1351-1383, 2003.
13. Mani SA, Guo W, Liao MJ, Eaton EN, Ayyanan A, Zhou AY, Brooks M, Reinhard F, Zhang CC, Shipitsin M, et al: The epithelial-mesenchymal transition generates cells with properties of stem cells. Cell 133: 704-715, 2008.
14. Liu Z, Sun B, Qi L, Li H, Gao J and Leng X: Zinc finger E-box binding homeobox 1 promotes vasculogenic mimicry in colorectal cancer through induction of epithelial-to-mesenchymal transition. Cancer Sci 103: 813-820, 2012.
15. Kalluri R and Weinberg RA: The basics of epithelial-mesenchymal transition. J Clin Invest 119: 1420-1428, 2009.
16. Bartel DP: MicroRNAs: Target recognition and regulatory functions. Cell 136: 215-233, 2009.
17. Fang L, Du WW, Yang W, Rutnam ZJ, Peng C, Li H, O'Malley YQ, Askeland RW, Sugg S, Liu M, et al: MiR-93 enhances angiogenesis and metastasis by targeting LATS2. Cell Cycle 11: 4352-4365, 2012.
18. Hu J, Xu J, Wu Y, Chen Q, Zheng W, Lu X, Zhou C and Jiao D: Identification of microRNA-93 as a functional dysregulated miRNA in triple-negative breast cancer. Tumour Biol 36: 251-258, 2015.

19. Chen S, Chen X, Sun KX, Xiu YL, Liu BL, Feng MX, Sang XB and Zhao Y: MicroRNA-93 promotes epithelial-mesenchymal transition of endometrial carcinoma cells. PLoS One 11: e0165776, 2016.
20. Shyamasundar S, Lim JP and Bay BH; SUKANYA S: miR-93 inhibits the invasive potential of triple-negative breast cancer cells *in vitro* via protein kinase WNK1. Int J Oncol 49: 2629-2636, 2016.
21. Livak KJ and Schmittgen TD: Analysis of relative gene expression data using real-time quantitative PCR and the 2(-Δ Δ C(T)) Method. Methods 25: 402-408, 2001.
22. Kim YK, Yu J, Han TS, Park SY, Namkoong B, Kim DH, Hur K, Yoo MW, Lee HJ, Yang HK, *et al*: Functional links between clustered microRNAs: Suppression of cell-cycle inhibitors by microRNA clusters in gastric cancer. Nucleic Acids Res 37: 1672-1681, 2009.
23. Li W, Liang L, He X, Wan D and Gu J: Study on the mechanism of hsa-miR93 in liver cancer. Weichangbingxue he Ganbingxue Zazhi 17: 478-480, 2008 (in Chinese).
24. Ambs S, Prueitt RL, Yi M, Hudson RS, Howe TM, Petrocca F, Wallace TA, Liu CG, Volinia S, Calin GA, *et al*: Genomic profiling of microRNA and messenger RNA reveals deregulated microRNA expression in prostate cancer. Cancer Res 68: 6162-6170, 2008.
25. Lowery AJ, Miller N, Devaney A, McNeill RE, Davoren PA, Lemetre C, Benes V, Schmidt S, Blake J, Ball G, *et al*: MicroRNA signatures predict oestrogen receptor, progesterone receptor and HER2/neu receptor status in breast cancer. Breast Cancer Res 11: 478-480, 2009.
26. Cascione L, Gasparini P, Lovat F, Carasi S, Pulvirenti A, Ferro A, Alder H, He G, Vecchione A, Croce CM, *et al*: Integrated microRNA and mRNA signatures associated with survival in triple negative breast cancer. PLoS One 8: e55910, 2013.
27. Nam EJ, Yoon H, Kim SW, Kim H, Kim YT, Kim JH, Kim JW and Kim S: MicroRNA expression profiles in serous ovarian carcinoma. Clin Cancer Res 14: 2690-2695, 2008.
28. Zhao X, Hu J and Zhao X: Screening of differentially expressed miRNA in triple negative breast cancer. Jiaotong University Xuebao 5: 569-571, 2012 (in Chinese).
29. Zhao X, Hu J and Zhao X: Expression and significance of hsa-miR-93 in triple negative breast cancer. Zhonghua Linchuang Yishi Zazhi 6: 3914-3916, 2012.
30. Weng C, Dong H, Chen G, Zhai Y, Bai R, Hu H, Lu L and Xu Z: miR-409-3p inhibits HT1080 cell proliferation, vascularization and metastasis by targeting angiogenin. Cancer Lett 323: 171-179, 2012.
31. Wu N, Zhao X, Liu M, Liu H, Yao W, Zhang Y, Cao S and Lin X: Role of microRNA-26b in glioma development and its mediated regulation on EphA2. PLoS One 6: e16264, 2011.
32. Shevde LA, Metge BJ, Mitra A, Xi Y, Ju J, King JA and Samant RS: Spheroid-forming subpopulation of breast cancer cells demonstrates vasculogenic mimicry via hsa-miR-299-5p regulated de novo expression of osteopontin. J Cell Mol Med 14 (6B): 1693-1706, 2010.
33. Sun T, Zhao N, Zhao XL, Gu Q, Zhang SW, Che N, Wang XH, Du J, Liu YX and Sun BC: Expression and functional significance of Twist1 in hepatocellular carcinoma: Its role in vasculogenic mimicry. Hepatology 51: 545-556, 2010.
34. Plantamura I, Casalini P, Dugnani E, Sasso M, D'Ippolito E, Tortoreto M, Cacciatore M, Guarnotta C, Ghirelli C, Barajon I, *et al*: PDGFRβ and FGFR2 mediate endothelial cell differentiation capability of triple negative breast carcinoma cells. Mol Oncol 8: 968-981, 2014.